

3D-QSAR of Non-peptidyl Caspase-3 Enzyme Inhibitors Using CoMFA and CoMSIA

Do Young Lee, Kwan Hoon Hyun, Hyung Yeon Park, Kyung A Lee, Bon-Su Lee, and Chan Kyung Kim*

Computer Aided Molecular Design Lab., Department of Chemistry, Inha University, Incheon 402-751, Korea

*E-mail: kckyoung@inha.ac.kr

Received August 8, 2005

Three dimensional quantitative structure-activity relationship studies for a series of isatin derivatives as a non-peptidyl caspase-3 enzyme inhibitor were investigated using comparative molecular field analysis (CoMFA) and comparative molecular similarity indices analysis (CoMSIA). The first approach of non-peptidyl small molecules by 3D QSAR may be useful in guiding further development of potent caspase-3 inhibitors.

Key Words : CoMFA, CoMSIA, 3D-QSAR, Caspase-3 inhibitors

Introduction

Apoptosis is one of the most common processes about cell death and is mediated by some proteases known as caspases.¹ The caspases (cysteiny aspartic proteases) are a family of cysteine proteases composed of at least 14 members and dysregulated caspases have been implicated in various disease states such as stroke, rheumatoid arthritis, and some tumors.^{2,3} Among them, caspase-3 enzyme plays a major role in the apoptotic signaling cascade and thus it may be a potential target for the treatment of the diseases caused by abnormal cell death.^{4,5}

Several peptide inhibitors and its mimetic compounds have been reported in the literature. Unfortunately, peptides are not well suited for therapeutic application because they have a short half-life and are unable to penetrate the blood-brain-barrier easily in most cases.⁶ However, Lee et al. have introduced conformationally constrained isatin sulfonamides as highly potent and selective caspases-3 and -7 inhibitors.⁷

In this work, we plan to perform QSAR study on non-peptidyl small molecular weight inhibitors using the 3D-QSAR to correlate their biological activities with three-dimensional structures and to provide useful information necessary for designing improved lead compounds. As far as we know, no such studies have been performed before. In general, 3D-QSAR studies have been applied successfully to provide useful information on the structure-activity relationships.⁸

Methods

Dataset for analysis. A data set of 25 compounds measured using standard fluorometric assay has been taken from the literature.⁷ Molecular structures and inhibitory activities (pIC_{50}) of the isatin derivatives are shown in Figure 1 and Table 1, respectively.

Computational methods. Calculations and statistical analyses were done on a LINUX (Redhat 6.9) PC (Intel Pentium 4 CPU) using SYBYL 6.9 software packages.⁹ All compounds were sketched using the sketch module in the SYBYL package and initially minimized using the standard

TRIPOS force field with Gasteiger-Hückel charge until the energy gradient converged below 0.001 kcal/mol.

All of these compounds were superimposed on a template, 1-methyl-5-(2-phenoxymethyl-pyrrolydone-1-sulfonyl)-1H-indole-2,3-dione (**20**) that was extracted from the X-ray structures of the caspases-3/isatin complex available on the protein data bank (PDB ID : 1GFW).¹⁰

Calculation of CoMFA descriptors. CoMFA was performed with the QSAR option of SYBYL.¹¹⁻¹⁵ For all

Table 1. Experimental, calculated inhibitory activities (pIC_{50}) and residuals of the training set molecules

Molecule	Experimental		Calculated pIC_{50}		Residuals	
	$IC_{50}(\mu M)$	pIC_{50}	CoMFA	CoMSIA	CoMFA	CoMSIA
1	1.0	6.00	5.62	5.82	0.38	0.18
2	0.25	6.60	6.58	6.58	0.02	0.02
3	3.0	5.52	5.64	5.65	-0.12	-0.13
4	100.0	4.00	4.02	4.07	-0.02	-0.07
5	15.0	4.82	4.90	4.87	-0.08	-0.05
6	0.6	6.22	6.34	5.92	-0.12	0.30
7	50.0	4.30	4.46	4.47	-0.16	-0.17
8	0.12	6.92	6.53	6.60	0.39	0.32
9	18.0	4.74	4.67	4.70	0.07	0.04
10	0.91	6.04	6.08	6.36	-0.04	-0.32
11	0.17	6.77	6.44	6.32	0.33	0.45
12	2.8	5.55	5.88	6.28	-0.33	-0.73
13	2.2	5.66	5.50	5.54	0.16	0.12
14	0.17	6.77	6.94	6.80	-0.17	-0.03
15	0.41	6.39	6.41	6.17	-0.02	0.22
16	0.031	7.51	7.63	7.49	-0.12	0.02
17	5.5	5.26	5.34	5.24	-0.08	0.02
18	0.044	7.36	7.47	7.53	-0.11	-0.17
19	0.044	7.36	7.50	7.22	-0.14	0.14
20	0.030	7.52	7.46	7.71	0.06	-0.19
21	0.0052	8.28	8.29	8.31	-0.01	-0.03
22	0.0025	8.60	8.49	8.46	0.11	0.14
23	0.0031	8.51	8.40	8.54	0.11	0.07
24	0.17	6.77	6.68	6.74	0.09	0.03
25	0.0042	8.38	8.57	8.46	-0.19	-0.08

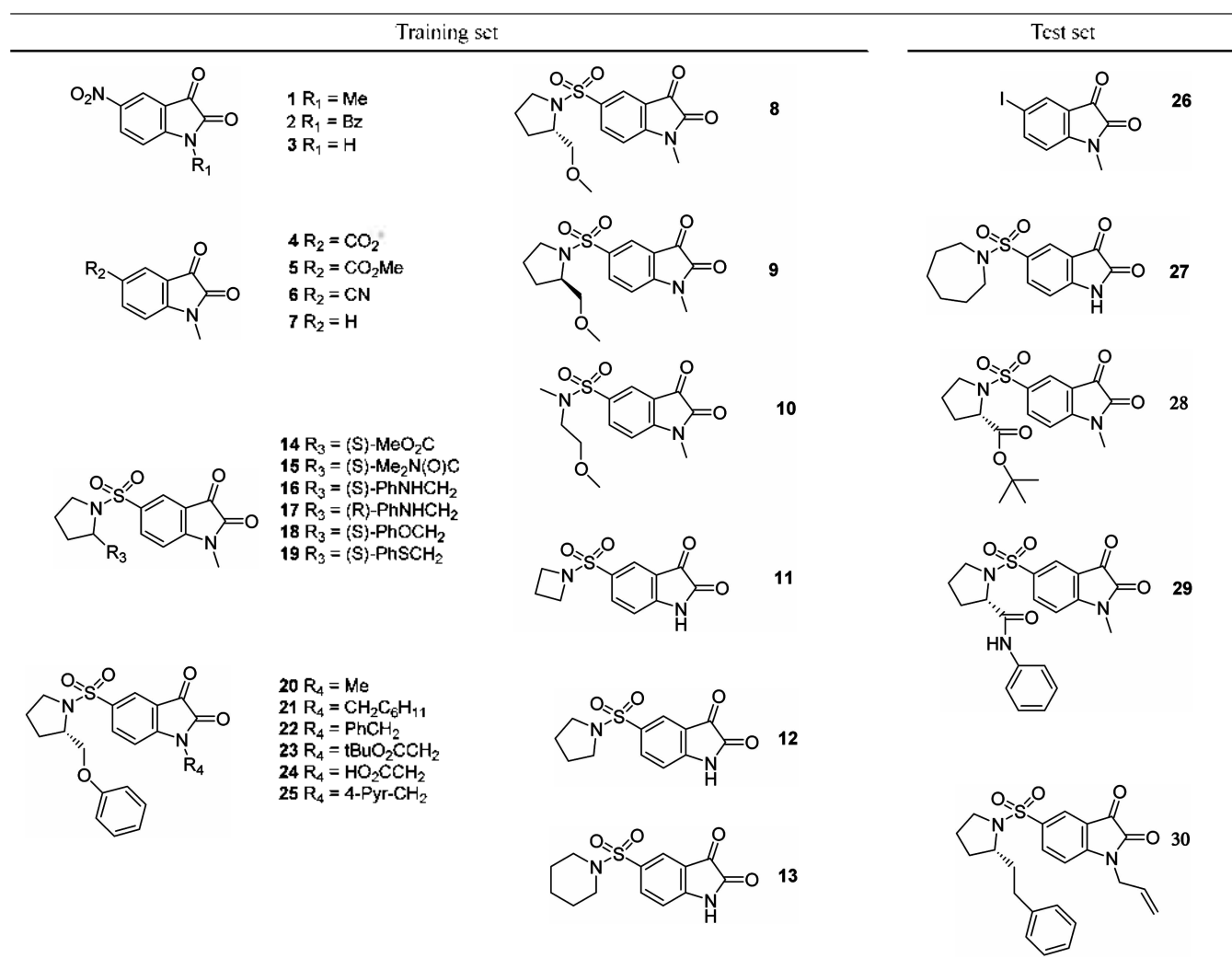


Figure 1. Data set used for 3D-QSAR analyses.

steps of conventional CoMFA, the default SYBYL settings were used. The steric (S) and electrostatic (E) field energies were calculated using sp^3 carbon probe atoms with +1 charge. CoMFA grid spacing used in this work was 2.0 Å in all X, Y and Z directions, and the QSAR equations were calculated with the partial least square (PLS) algorithm. Values of the steric and electrostatic energy were truncated at 30 kcal/mol.

Calculation of CoMSIA descriptors. In addition to the fields used in CoMFA method, the CoMSIA method provides hydrophobic (H) and H bond donor (D) and acceptor (A) fields.¹⁴ Grid spacing used in this work was 2.0 Å same as in CoMFA study. A probe atom with radius 1.0 Å and +1.0 charge with hydrophobicity of +1.0 and hydrogen bond donor and H bond properties (donor and acceptor) of +1.0 was used to calculate steric, electrostatic, hydrophobic, and H bond fields, respectively.

Alignment rule. Compound **20** was provided as the template and the other compounds were aligned to it using the FIT command in the SYBYL, as shown in Figure 2.

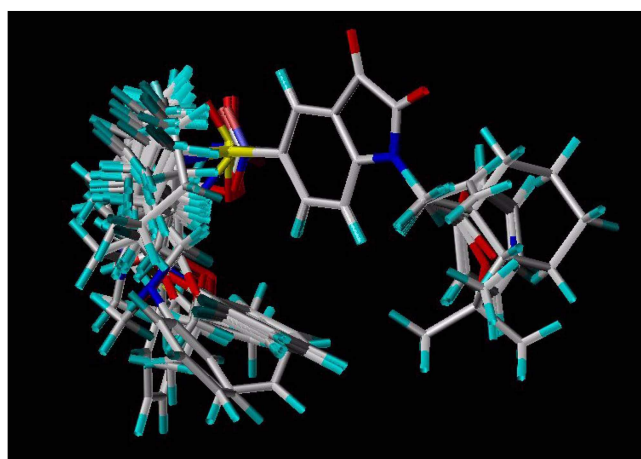


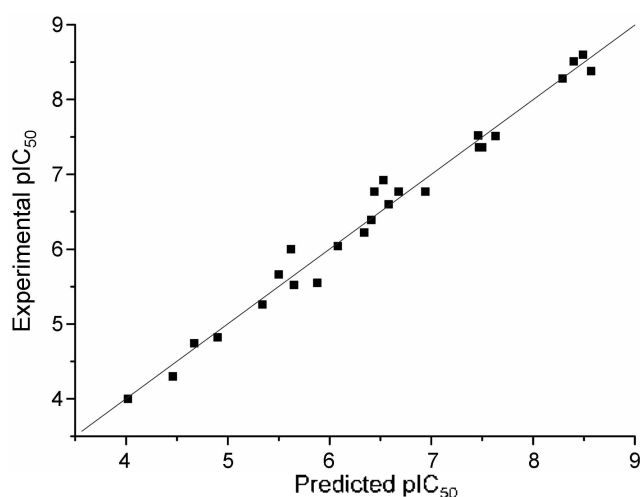
Figure 2. Alignments of the training set molecules.

Results and Discussion

The statistical results of the CoMFA and CoMSIA analyses are shown in Table 2. Both models were obtained

Table 2. Analysis of CoMFA and CoMSIA statistics

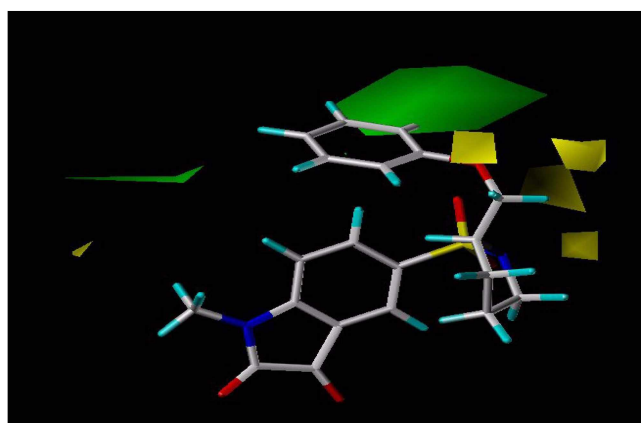
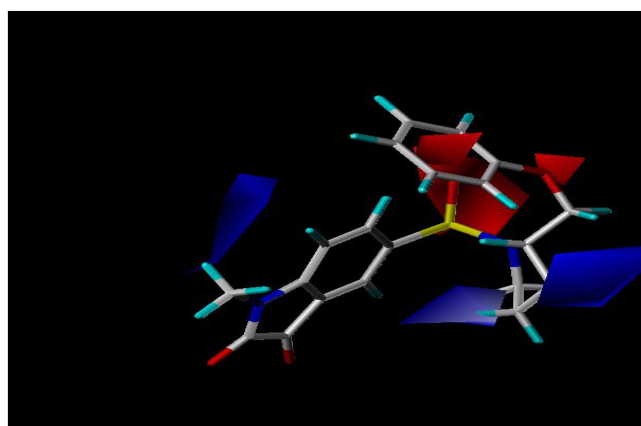
Parameter	CoMFA	CoMSIA			
		S+E	S+E+H	S-E+D+A	All
r^2_{cv}	0.698	0.707	0.734	0.773	0.719
ONC	5	5	5	6	6
r^2_{nev}	0.981	0.967	0.967	0.968	0.959
SEE	0.201	0.266	0.267	0.262	0.296
F	198.469	111.767	110.335	114.889	89.508
Contributions (%)					
Steric	0.491	0.334	0.210	0.251	0.180
Electrostatic	0.509	0.666	0.493	0.392	0.342
Donor				0.184	0.131
Acceptor				0.173	0.161
Hydrophobic			0.297		0.186

**Figure 3.** Plot of predicted versus actual pIC_{50} of training set molecules in CoMFA model.

with 25 molecules in training set and 5 molecules in test set. Inspection of Table 2 shows that leave-one-out cross-validated value (r^2_{cv}) is 0.698 and non cross-validated conventional value (r^2_{nev}) is 0.981 for CoMFA, which can suggest good prediction for caspase-3 inhibitor activities of the test set. The contribution of steric and electrostatic field was 49.1 and 50.9%, respectively. A plot of experimental versus predicted pIC_{50} values of the training set molecules

Table 3. Measured and predicted activities of five compounds in the test set using CoMFA and CoMSIA

compound	Measured pIC_{50}	CoMFA		CoMSIA	
		Predicted pIC_{50}	Residual	Predicted pIC_{50}	Residual
26	5.15	5.37	0.22	4.69	-0.46
27	5.72	5.39	-0.33	6.04	0.32
28	7.15	7.38	0.23	6.97	-0.18
29	6.85	6.80	-0.05	5.89	-0.96
30	8.34	7.69	-0.65	7.74	-0.60
Average			0.30		0.50

**Figure 4.** Steric field of CoMFA contour map. Sterically favored region is shown in green and sterically disfavored region is in yellow.**Figure 5.** Electrostatic field of CoMFA contour map. The positive charge favored regions are shown in blue and the negative charge favored regions are shown in red.

shows good linearity as depicted in Figure 3. To further validate our results, five compounds (**26-30**) with pIC_{50} range between 5.2 and 8.3 were assigned as test set and their biological activities were predicted from the PLS equations derived from CoMFA. Actual and predicted activities along with residual values are shown in Table 3.

Graphical representations of CoMFA results are shown in Figures 4 and 5 as 3D contour maps. The CoMFA steric and electrostatic maps are illustrated in Figures 4 and 5, respectively. The template molecule is displayed in the background of contours. Sterically favored region (in green) located in the vicinity of phenoxy group is originated from the bulky aromatic groups at R_3 (**16**, **18**, and **19**). Sterically unfavorable region (in yellow), which is found at the oxygen of phenoxy group, is caused by the displacement of this atom by inversion at the stereogenic center (S to R). The positively charged substituents are favored in blue regions and the negative ones are favored in red regions in Figure 5. The red contours near C_5 of isatin ring of the template molecule indicate that incorporation of electronegative substituents at R_2 enhances the inhibitory activity. The three blue contours are found in the electrostatic map – one near

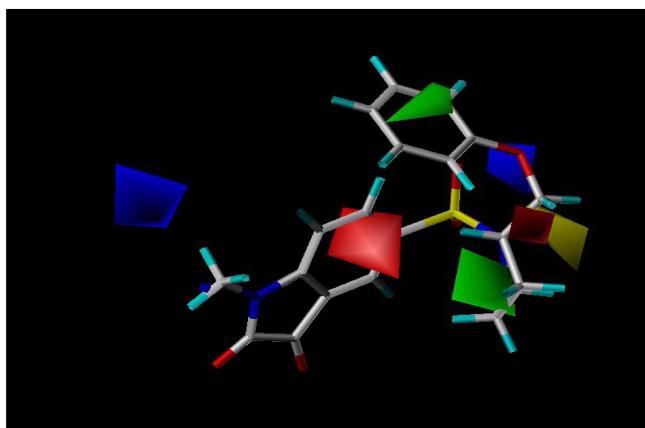


Figure 6. Steric and electrostatic fields of CoMSIA map. CoMSIA Color maps are represented using the same colors as those used for CoMFA maps.

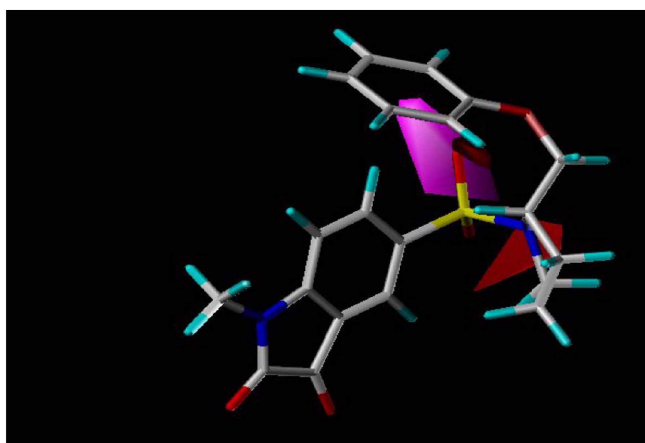


Figure 7. Hydrogen bond acceptor field of CoMSIA contour map. Magenta colored region is associated with enhanced affinity and red colored region is associated with diminished affinity with hydrogen bond acceptor substituents.

R₄ position is caused by the electron withdrawing CH₂CO₂H group and the other two regions are originated from the conformers with R configuration at the stereogenic center (9 and 17).

The CoMSIA results were obtained with four different combinations of fields using the same data set as CoMFA. The r^2_{ncv} from CoMSIA is slightly lower than that of CoMFA but the r^2_{cv} showed opposite trend. Among them, the best statistical results were from the combination of four fields (S + E + D + A) with r^2_{cv} 0.773 (the contribution ratios were 25.1, 39.2, 18.4, and 17.3%, respectively). The contribution of these fields is depicted in Figures 6 and 7. Two sterically favored regions are found – one near the phenoxy group is the same as found in the CoMFA map and another region in the vicinity of the pyrrolidone ring is originated from sterically demanding substituents such as acyclic alkyl chains (10) to four-membered ring (11) and five-membered ring (for example, 8). Electrostatically favored region (in red) found at C₅ position of isatin ring is caused by electron withdrawing substituents at this position

(1, 5 vs. 7). Two electrostatic disfavored regions found at R₄ and phenoxy oxygen came from electron withdrawing CH₂COOH group (24) and displaced oxygen atom by inversion of the stereochemistry (9 and 17). The hydrogen bond donor and acceptor map is shown in Figure 7. In this CoMSIA map, it is obvious that the contribution by hydrogen bond donor region does not appear in the map since there are no such atoms in the training set molecules. The magenta contour suggests that the hydrogen bond acceptor substituent, -SO₂, enhances the inhibitory activity. Compounds 1-7, which have no hydrogen bond acceptor nitrogen, show worse activity than other compounds having a pyrrolidine ring and this is shown in red in Figure 7.

Conclusion

The 3D QSAR studies were performed for a series of isatin derivatives with inhibitory activity on the caspase-3 enzyme using CoMFA and CoMSIA. Both CoMFA and CoMSIA models with Gasteiger-Hückel charge were exhibited a good correlation with experimental results. From above PLS correlations, activities of five test set molecules were predicted satisfactorily. The first approach of non-peptidyl small molecules by 3D QSAR may be useful for guiding further development of potent caspase-3 inhibitors.

Acknowledgement. This work was supported by INHA UNIVERSITY Research Grant.

References

- Talanian, R. V.; Brady, K. D.; Cryns, V. L. *J. Med. Chem.* **2000**, *43*, 3351
- Thornberry, N. A.; Lazebnik, Y. *Science* **1998**, *281*, 1312
- Eamshaw, W. C. *Annu. Rev. Biochem.* **1999**, *68*, 383.
- Porter, A. G.; Janicke, R. U. *Cell Death Differ.* **1999**, *6*, 99.
- Nicholson, D. W.; Thornberry, N. A. *Trends Biochem. Sci.* **1997**, *22*, 299.
- Estiarte, M. A.; Rich, D. H. *Burger's Medicinal Chemistry and Drug Design*, 6th ed.; 2003; Vol. 1, p 633.
- Lee, D.; Long, S. A.; Murray, J. H.; Adams, J. L.; Nuttall, M. E.; Nadeau, D. P.; Kikly, K.; Winkler, J. D.; Sung, C.-M.; Ryan, M. D.; Levy, M. A.; Keller, P. M.; DeWolf, W. E. Jr. *J. Med. Chem.* **2001**, *44*, 2015.
- (a) Hyun, K. H.; Kwack, I. Y.; Lee, D. Y.; Park, H. Y.; Lee, B.-S.; Kim, C.-K. *Bull. Korean Chem. Soc.* **2004**, *25*, 1801. (b) San Juan, A. A.; Cho, S. J. *Bull. Korean Chem. Soc.* **2005**, *26*, 952.
- SYBYL Molecular Modeling Software; Tripos Inc.: St. Louis, MO 63144, U.S.A.
- Lee, D.; Chan, G.; Vaidya, K. S.; Francis, T. A.; Nadeau, D. P.; Lark, M. W.; Gowen, M.; Kikly, K.; Winkler, J. D.; Sung, C.-M.; Long, S. A.; Adams, J. L.; Debouck, C.; Richardson, S.; Levy, M. A.; Dewolf, W. E., Jr.; Keller, P. M.; Tomaszek, T.; Head, M. S.; Ryan, M. D.; Haltiwanger, R. C.; Liang, P.-H.; Janson, C. A.; Medevi, P. J. *J. Biol. Chem.* **2000**, *275*, 16007.
- Hansch, C.; Leo, A. In *Exploring QSAR*; American Chemical Society: Washington DC, 1995.
- Cramer, R. D.; Patterson, D. E.; Bunce, J. D. *J. Am. Chem. Soc.* **1988**, *110*, 5959.
- Dean, P. M. In *Molecular Similarity in Drug Design*; Blackie Academic & Professional: Glasgow, 1995, p 291.
- Klebe, G.; Abraham, U.; Mietzner, T. *J. Med. Chem.* **1994**, *37*, 4130.